available at www.sciencedirect.com

ScienceDirect

journal homepage: www.ejconline.com

Preclinical evaluation of vascular-disrupting agents in Ewing's sarcoma family of tumours ☆

*Surita Dalal**, *Susan A. Burchill*

Candlelighter's Children's Cancer Research Group, Cancer Research UK Clinical Centre, Leeds Institute of Molecular Medicine, St. James's University Hospital, Beckett Street, Leeds, West Yorkshire LS9 7TF, UK

ARTICLE INFO

Article history:
Received 10 April 2008
Received in revised form
21 November 2008
Accepted 24 November 2008
Available online 10 January 2009

Keywords:
Ewing's sarcoma
Angiogenesis
Vasculature
Combretastatins
Doxorubicin

ABSTRACT

The effects of the tubulin-binding vascular-disrupting agents (VDAs), combretastatin A4 phosphate (CA4P), OXi4503/CA1P and OXi8007, in subcutaneous mouse models of the Ewing's sarcoma family of tumours (ESFTs) have been investigated alone and in combination with doxorubicin. Delay in subcutaneous tumour growth was observed following treatment of mice with multiple doses of OXi4503/CA1P but not with CA4P or OXi8007. A single dose of OXi4503/CA1P caused complete shutdown of vasculature by 24 h and extensive haemorrhagic necrosis by 48 h. However, a viable rim of proliferating cells remained, which repopulated the tumour within 10 days following the withdrawal of treatment. Combined treatment with doxorubicin 1 h prior to administration of OXi4503/CA1P enhanced the effects of OXi4503/CA1P causing a synergistic delay in tumour growth ($p < 0.001$). This study demonstrates that OXi4503/CA1P is a potent VDA in ESFT and in combination with conventional cytotoxic agents represents a promising treatment strategy for this tumour group.

1. Introduction

Tumours of the Ewing's sarcoma family (ESFT) are poorly differentiated small round cell tumours, characterised by the presence of non-random chromosomal translocations between the *EWS* gene on chromosome 22q12 and members of the *ETS* gene family.[1] ESFT predominantly occur in children and adolescents between the ages of 10 and 20 years, 20–30% presenting with metastatic disease.[2,3] Despite recent advances in multimodal treatment, the 5-year survival for such patients remains poor; less than 30% for patients with metastatic disease and 60% for patients with localised disease.[4,5] This emphasises the need for new therapeutic strategies in this disease group.

It is now well established that tumours exceeding 2–3 mm in size need to initiate the process of angiogenesis for growth and progression,[6] and that this process is a good target for the development of novel therapeutics. Currently, two key strategies exist for targeting tumour vasculature: anti-angiogenic compounds that target neovascularisation (most widely investigated) and vascular disruption, which selectively targets pre-existing tumour vasculature to cause rapid decrease in blood flow and subsequent ischaemic or haemorrhagic necrosis of tumour.[7] There are two classes of vascular-disrupting agents (VDAs): small molecule VDAs and ligand-directed VDAs. Small molecule VDAs, such as the combretastatins, are designed to achieve vascular shutdown by exploiting the abnormal characteristics of tumour blood vessels.[7] Combretastatins such as combretastatin A-4 disodium phosphate prodrug (CA4P), OXi4503/CA1P and AVE8062 all function as microtubule-destabilising agents, binding tubulin at or near the colchicine binding site.[8,9] Susceptibility of the proliferating and immature tumour endothelial cell to these compounds most likely reflects their increased vascular permeability and

☆ Grant information: This work was funded by the Candlelighter's Trust, Leeds, United Kingdom and OXiGENE Inc., USA.
* *Corresponding author:* Tel.: +44 113 206 8104/7851; fax: +44 113 2067883.
E-mail address: s.dalal@leeds.ac.uk (S. Dalal).
0959-8049/$ - see front matter © 2008 Elsevier Ltd. All rights reserved.
doi:10.1016/j.ejca.2008.11.045

reliance on the tubulin cytoskeleton to maintain the endothelial morphology.[10,11] The OXiGENE Inc. lead combretastatin CA4P is a soluble tris phosphate prodrug, cleaved to its active form (CA4) by endogenous non-specific phosphatases.[12] More recently, a more potent second generation tubulin-binding agent OXi4503/CA1P, the diphosphate prodrug of CA1, has been described.[13] Although structurally related to CA4P, this compound more effectively inhibits functional vasculature and tumour growth in various animal models.[9,14,15] Both CA4P and OXi4503/CA1P are currently undergoing clinical trials either as single agents or in combination with conventional therapeutics (http://www.oxigene.com/vascular/vascular.asp#VDATECH). OXi8007 is a combretastatin analogue that exhibits potent anti-vascular activity in preclinical studies.[16]

As in many tumours, tumour vasculature plays an important role in the development and progression of ESFT.[17,18] The rapid shutdown of existing vasculature and subsequent secondary tumour cell necrosis induced by tubulin-binding agents such as combretastatins highlight these agents as ideal candidates for the acute treatment of patients with large, metastatic tumours which are usually less responsive to conventional therapies.[19] At diagnosis, over 60% of ESFT patients present with large tumours (>100 ml) and 20–30% with detectable metastatic disease, both of which are indicators of poor outcome,[2] making them prime candidates for vascular-disrupting therapy.[20] However, to date the effect of VDAs has not been investigated in ESFT.

The primary aim of this study was to investigate and compare the preclinical effects of the combretastatins CA4P, OXi4503/CA1P and OXi8007 using two ESFT subcutaneous growth models (TC-32 and A673) in nude mice. The effects of the combretastatins on tumour growth, histology, microvessel density (MVD) and perfused vascular volume have been described alone and in combination with doxorubicin (used to treat ESFT).

2. Materials and methods

2.1. Compounds

CA4P, OXi4503/CA1P and OXi8007 (OXiGENE, Inc. Waltham, MA, USA) and doxorubicin (Sigma) were prepared in 0.9% saline immediately prior to use. Saline (0.9%) was the vehicle control.

2.2. Cell lines

TC-32 cells were grown in RPMI 1640 media (Sigma) containing 10% FCS (Harlan Sera-Lab Ltd.), and A673 cells were grown in Dulbecco's Modified Eagle's Media (Sigma) containing 10% FCS.

2.3. Subcutaneous tumours and drug treatment

Immunocompromised *nu/nu* mice aged 6–8 weeks were injected subcutaneously in one flank with TC-32 or A673 cells (5×10^6 cells/0.2 ml of media). All animals were housed under 12 hourly cycles of light and darkness in an air-conditioned room, and had unrestricted access to water and food. On day 15, following the development of a palpable tumour, mice ($n = 4$–5) were randomised into different treatment groups; all treatments (CA4P 100 mg/kg; OXi4503 25 mg/kg; OXi8007 200 mg/kg; Doxorubicin 5 mg/kg) were given intraperitoneally, and the vehicle control used was 0.9% NaCl. Group 1: twice weekly dosing of mice with TC-32 or A673 tumours with either CA4P, OXi4503, OXi8007 or vehicle control for up to three weeks. Mice with TC-32 tumours treated with OXi4503 were maintained for a further 10 days after the treatment had been stopped. Group 2: mice with TC-32 tumours treated with a single dose of either CA4P, OXi4503, OXi8007 or vehicle control for 24 or 48 h. Group 3: twice weekly dosing of mice with TC-32 tumours with either OXi4503 or Doxorubicin, Doxorubicin followed 1 h later with OXi4503 or vehicle control for up to two weeks.

Tumour growth was measured twice weekly using callipers in two directions, the largest diameter (a) and its perpendicular (b) (tumour size = $a \times b$). Mice were sacrificed when tumours reached a size of 1.4 cm^2, at the end of the experiment or if the mice showed signs of distress. All procedures were performed under Home Office Licence number PPL 70/5260, in accordance with the guidelines for the welfare of animals in experimental neoplasia.[21]

2.4. Histological and Immunohistochemical analyses

Following the different drug treatments described above, subcutaneous tumours were excised and divided into two groups. Half were fixed in zinc fixative (BD Biosciences) and embedded in paraffin, the other half were embedded in OCT compound and frozen in liquid nitrogen. The histology of paraffin-embedded tumour sections (4 μm) was examined by staining with H&E and by light microscopy. Immunohistochemistry for CD31, GLUT-1 and Ki67, and TUNEL were performed on serial sections (4 μm) of treated and control tumours to identify vascular endothelial cells, hypoxic, proliferating and apoptotic cells, respectively. A serial section was processed without target specific primary antibody to test for non-specific binding (negative control).

CD31 was detected using a three-stage peroxidase method as per the manufacturer's instructions; Vectastain Elite ABC Kit (Vector Laboratories). Briefly antigen retrieval was performed by incubating sections in boiling citric acid buffer (10 mM citric acid, pH 6) for 12 min. Sections were then incubated in peroxidase block (0.3% H_20_2; Sigma) for 30 min, followed by incubation in Avidin/Biotin block (10 min per solution; Vector Laboratories) and finally in normal blocking serum for 20 min. Sections were then incubated with goat anti-human CD31 primary antibody (SC-1506; Santa Cruz Biotechnology) at 1:100 for 1 h. After rinsing twice in phosphate buffered saline (PBS), sections were incubated with Vectastain® biotinylated anti-goat IgG for 30 min. After two further washes in PBS, sections were incubated with Vectastain Elite ABC reagent for 30 min and rinsed twice with PBS, and staining was visualised following incubation with 3,3′diaminobenzidine (DAB; Vector Laboratories) substrate for 10 min; staining was visible as brown precipitate. Sections were rinsed for 1 min in running water and counterstained using haematoxylin.

GLUT-1 expression was detected using a three-stage peroxidase method similar to that described for CD31. Following

the blocking steps (described above), sections were incubated with normal goat serum (DakoCytomation Ltd.), diluted 1:10 in PBS for 1 h. Sections were then incubated with rabbit anti-human GLUT-1 primary antibody (A3536; DakoCytomation Ltd.) at 1:50 for 1 h, rinsed twice in PBS and then incubated with biotinylated goat anti-rabbit IgG secondary antibody (DakoCytomation Ltd.), diluted 1:200 in PBS for 30 min. After two further washes in PBS, sections were incubated with streptABcomplex (StreptABcomplex/HRP Kit; DakoCytomation Ltd.) for 30 min, rinsed twice with PBS and visualised as described above.

Ki67 was detected using the Vector® M.O.M.™ Immunodetection Kit (Vector Laboratories) as per the manufacturer's instructions. Antigen retrieval and blocking steps were carried out as described above. Prior to incubation with primary antibody, M.O.M.™ blocking reagent was applied to sections for 1 h, followed by two rinses in PBS and incubation in M.O.M.™ diluent for a further 5 min. Sections were incubated with mouse anti-human Ki67 primary antibody (M-7240; DakoCytomation Ltd.) at 1:50 for 30 min. After rinsing twice in PBS, the sections were incubated with M.O.M.™ biotinylated anti-mouse IgG for 10 min, washed twice in PBS, incubated with streptABcomplex for 30 min, rinsed again with PBS and visualised as described above.

For detection of apoptotic cells the terminal deoxynucleotidyl transferase-mediated nick-end labelling (TUNEL) assay was performed using the ApopTag® *In Situ* Apoptosis Detection Kit (CHEMICON International, Inc.), according to the manufacturer's instructions.

2.5. Determination of micro-vessel density (MVD) and proliferation index

Following staining with CD31, each section was scanned on a Zeiss Axioplan microscope at x160 magnification to identify three areas with the greatest MVD. The vessel count was performed at ×250 magnification for an overall area of 0.79 mm^2 for each of the three 'hotspots' identified and the mean micro-vessel count was calculated. MVD was expressed as the number of micro-vessels per mm^2. Following staining with Ki67, four viable areas in each section were randomly selected and Ki67-positive cells in a total of a hundred cells for each field were counted at ×250 magnification. To determine the proliferation index, the mean Ki67 count was calculated and proliferation index was calculated (number of Ki67-positive cells ÷ number of cells counted) × 100.

2.6. Hoechst 33342 studies

Perfused vasculature was identified using the fluorescent DNA-binding compound Hoechst 33342 (Sigma). Following i.v. injection, vascular endothelial cells have been shown to rapidly and stably incorporate Hoechst 33342, thus allowing identification of perfused vessels within the tumour bed.[22]

Mice were injected with TC-32 cells as described above. On day 15, following the development of a palpable tumour, mice ($n = 4–5$) were randomised into two different treatment groups (OXi4503 25 mg/kg; Doxorubicin 5 mg/kg); all treatments were given intraperitoneally, and vehicle control used was 0.9% NaCl. Group 1: treatment with a single dose of OXi4503 or vehicle control for 1, 24 or 48 h. Group 2: treatment with a single dose of OXi4503 or Doxorubicin, Doxorubicin followed 1 h later with OXi4503 or vehicle control for 1, 24 or 48 h. Hoechst 33342 (40 mg/kg) was dissolved in saline and injected intravenously (5 ml/kg) into the tail vein 1, 24 or 48 h after treatment.[22] Mice were sacrificed 1 min later, and tumours were excised, wrapped in foil and frozen immediately by immersing in liquid nitrogen. Serial sections (10 μm) of whole tumours were prepared using a cryostat and were mounted on glass slides; sections from three different depths (upper third, middle third and lower third) within each tumour were scored. Before observing under UV illumination, sections were fixed in acetone (1 min), air dried and mounted in faramount (DakoCytomation Ltd.), and then scanned (×200 magnification) using an Axiovert 200 M microscope (Carl Zeiss) fitted with a motorised stage. Composite images were generated from multiple fields captured for each section using the imaging software programme Volocity (Version 3.7; Improvision Ltd., Coventry, UK). Nine random fields were scored for each of the three sections. Perfused vasculature was observed as fluorescence and was quantified using a 25 × 19 graticule grid.[14]

2.7. Statistics

The effect of VDAs on subcutaneous tumour growth were analysed using a two-stage regression. A linear regression was fitted to each mouse-specific tumour growth curve and the slope coefficients (which estimate the average tumour growth rate in each mouse) were used as the dependent variable in an analysis of covariance comparing treatments, with and without the starting tumour size as a covariate.

MVD was analysed using one-way analysis of variance of the treatment for each experiment and time point. Where there was an overall statistically significant treatment effect (*F* Test), pairwise differences between treatment groups were compared using modified *t*-tests.

Perfused vascular volume was analysed using a mixed effects analysis of variance, taking mice as independent subjects and comparing averaged scores between mice. Analyses were carried out on the natural Log(score +1), but were reported on the back-transformed (original) scale. A p-value < 0.05 was considered significant for all studies.

3. Results

3.1. Effect of CA4P, OXi4503/CA1P and OXi8007 on s.c. growth of ESFT

Significant delay in TC-32 tumour growth was observed following treatment of mice with OXi4503/CA1P (25 mg/kg/twice weekly; $p < 0.001$) when compared to the growth of tumours treated with vehicle only (Fig. 1A). Although some delay was observed in tumours treated with CA4P (100 mg/kg/twice weekly), this failed to achieve statistical significance (Fig. 1A). No delay in growth was observed in tumours treated with OXi8007 (200 mg/kg/twice weekly) (Fig. 1A). Similarly, in the A673 tumours a delay in tumour growth was observed following treatment with OXi4503/CA1P (25 mg/kg/twice weekly; $p = 0.14$), but not following treatment with other compounds

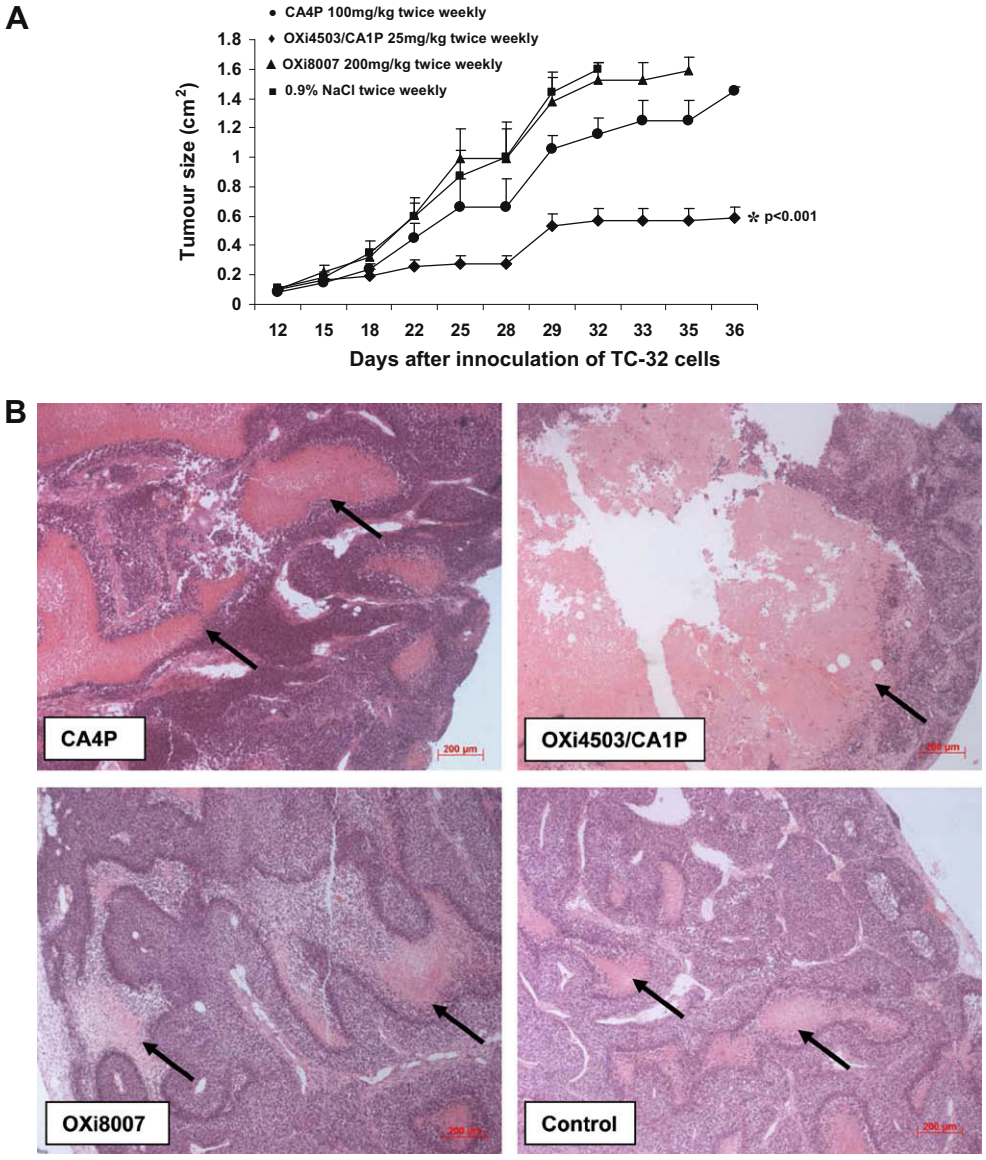

Fig. 1 – (A) Multiple dosing with OXi4503/CA1P but not CA4P or OXi8007 significantly delayed subcutaneous TC-32 growth ($n = 3–5$). (B) H&E staining of excised tumours demonstrated extensive areas of necrosis following treatment of mice with OXi4503/CA1P (necrosis ↑). ×40 magnification.

(results not shown). Histological examination of tumours revealed extensive necrosis following treatment with OXi4503/CA1P when compared to control tumours (Fig. 1B). There was no increase in necrosis of tumours from mice treated with CA4P or OXi8007 compared to control vehicle only-treated mice (Fig. 1B). All compounds that were delivered alone were well tolerated by mice.

3.2. *Early effects of CA4P, OXi4503/CA1P and OXi8007 on histology and vasculature*

Histological examination of TC-32 tumours that were excised after 24 h and stained with H&E revealed an increase in necrotic areas in CA4P-, OXi4503/CA1P- and OXi8007-treated mice when compared to control vehicle only-treated mice (Fig. 2). This effect was most pronounced in mice treated with OXi4503/CA1P (Fig. 2). Vessel occlusion was observed in areas of necrosis within each treatment group, although this was most extensive in tumours from mice treated with OXi4503/CA1P (Fig. 2). Tumours in OXi4503/CA1P-treated mice were more vacuolated at 48 h compared to those at 24 h (Fig. 2). In contrast, only small areas of necrosis were observed in CA4P- and OXi8007-treated mice (results not shown).

No change in MVD (micro-vessels/mm^2) was observed in the TC-32 tumours 24 h after a single dose of CA4P (77.33 ± 16.93), OXi4503/CA1P (58.47 ± 4.13) or OXi8007 (67.73 ± 6.98) when compared to control tumours (70.33 ± 2.52). CD31-positive endothelial cells/blood vessels were present throughout the viable areas in all tumour groups despite histological evidence of vessel shutdown (Fig. 2). In contrast, MVD was decreased in tumours from OXi4503/CA1P-treated mice after 48 h (Fig. 3A and B; $p = 0.004$). In these mice, disruption of

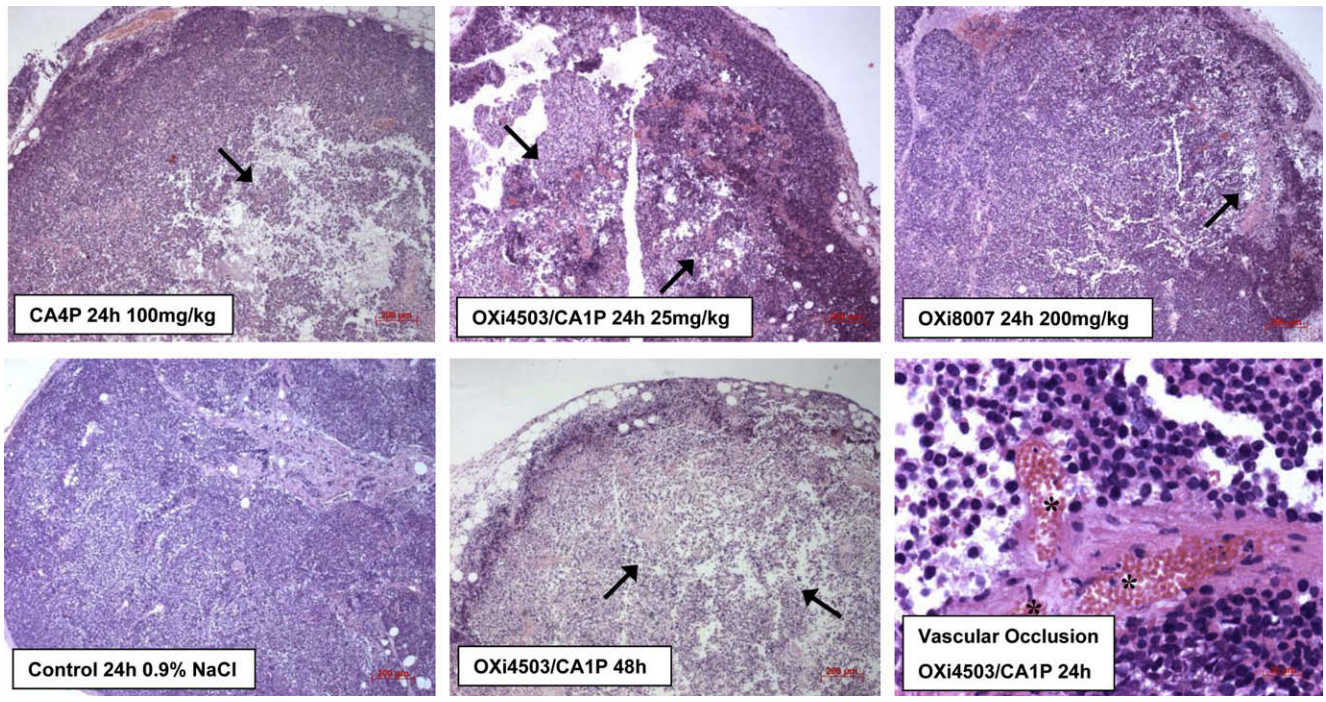

Fig. 2 – Extensive necrosis was observed in TC-32 tumours following treatment with a single dose of OXi4503/CA1P, compared to CA4P-, Oxi8007- or vehicle control-treated mice (necrosis ↑; ×40 magnification). Vascular occlusion (*; ×400 magnification) was predominantly observed in OXi4503/CA1P-treated tumours.

the vasculature was evident with smaller blood vessels or single EC largely confined to the viable periphery of these tumours (Fig. 3A). This effect was not observed in tumours from CA4P-or OXi8007-treated mice (Fig. 3A and B).

3.3. *Early effects of OXi4503/CA1P on perfused vascular volume*

Significant effects on perfused vascular volume were observed as early as 1 h post treatment with OXi4503/CA1P, with a 75% reduction in perfused vasculature in tumours from treated mice compared to that of control tumours (Fig. 4A and B; $p < 0.001$). At 24 h, vascular shutdown was almost 100% (Fig. 4A and B; $p < 0.001$ compared to control). By 48 h, some recovery of the vasculature was observed at the viable periphery of the tumour (Fig. 4A and B). Consistent with the observations described above for CD31 at 48 h, the perfused vessels appeared smaller compared to those identified in tumours from control mice.

3.4. *Early effects of OXi4503/CA1P on hypoxia*

Upregulation of GLUT-1, a marker of hypoxia, was observed in tumours 24 h and 48 h after a single treatment with OXi4503/CA1P. Compared to control tumours, where GLUT-1 was expressed throughout the tumour, strong expression of GLUT-1 was predominantly membrane localised at the periphery of tumours from treated mice (results not shown). In addition to the peripheral staining, upregulation of GLUT-1 expression was also observed in the endothelial cell lining of tumour blood vessels in OXi4503/CA1P-treated mice.

3.5. *Early effects of single dose CA4P, OXi4503/CA1P and OXi8007 on proliferation and apoptosis*

No difference in the proliferation index of TC-32 tumours was observed 24 h following treatment of mice with a single dose of CA4P (49.90 ± 2.50), OXi4503/CA1P (40.35 ± 5.88) or OXi8007 (44.45 ± 4.40) compared to that in control (45.33 ± 5.08)-treated mice. Despite an increase in the amount of necrosis in tumours from mice treated for 48 h, no further difference was observed with CA4P (47.15 ± 4.33), OXi4503/CA1P (41.88 ± 4.29) or OXi8007 (44.90 ± 8.84) compared to the tumours from control (46.44 ± 2.57) mice. In all groups, Ki-67-positive cells were observed in the viable areas of the tumours but were absent in the necrotic areas (results not shown).

There was no difference in apoptotic cell number detected by TUNEL 24 h following treatment of mice. In tumours from both treated and control mice, TUNEL-positive apoptotic cells were observed in the area adjacent to necrotic cells but were virtually absent in other regions of the tumour (results not shown). Although there was an increase in the number of TUNEL-positive cells in TC-32 tumours 48 h following treatment with a single dose of CA4P and OXi4503/CA1P compared to control tumours, positive cells were again confined to the area immediately surrounding necrotic cells.

3.6. *Effect of combined treatment with OXi4503/CA1P and doxorubicin on growth of s.c. ESFT*

Despite the extensive necrosis observed following treatment of mice with OXi4503/CA1P, approximately 10 days after the

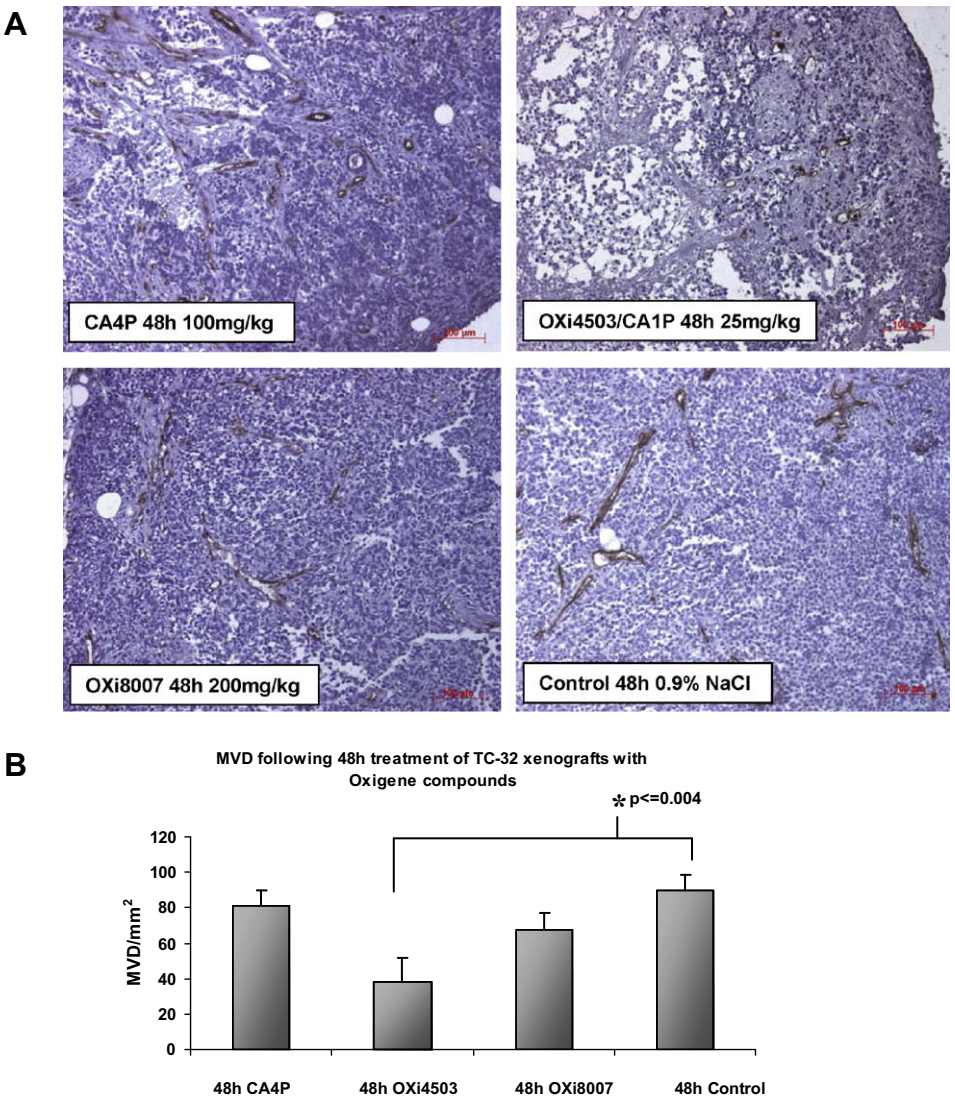

Fig. 3 – (A) CD31 immunolabelling of TC-32 tumours 48 h after treatment of mice with a single dose of CA4P, OXi4503/CA1P, OXi8007 or vehicle control (×100 magnification). (B) Significant reduction in MVD was observed in OXi4503/CA1P-treated tumours compared to other groups ($n = 4–5$).

withdrawal of OXi4503/CA1P (day 36; Fig. 5A) all tumours in this group rapidly re-grew (>1.4 cm^2), consistent with the rapid proliferation of the rim of viable cells that remained after treatment (Fig. 5B). We therefore hypothesised that improved inhibition of tumour growth might be achieved by treating mice with the cytotoxic agent doxorubicin in combination with OXi4503/CA1P. Consistent with the previous observations, growth of TC-32 tumours was delayed following treatment of mice with OXi4503/CA1P or doxorubicin alone (Fig. 6; $p < 0.001$). However, when given in combination (doxorubicin 1 h prior to treatment with OXi4503/CA1P), a significant synergistic delay in tumour growth was observed (Fig. 6; $p < 0.001$ combined treatment versus control; $p = 0.002$ combined treatment versus OXi4503/CA1P alone; $p = 0.03$ combined treatment versus doxorubicin alone). Histological examination of tumours from mice treated with OXi4503/CA1P plus doxorubicin revealed extensive areas of necrosis (consistent with the effects of OXi4503/CA1P) and importantly a reduced viable proliferative rim of tumour cells compared to tumours from mice treated with OXi4503/CA1P alone (results not shown). Unfortunately, further treatment (i.e. beyond two weeks) with the combination of doxorubicin and OXi4503 was not well tolerated by the mice, and the experiment had to be stopped following 5–6 combined treatments.

3.7. *Effect of combined treatment of mice with OXi4503/CA1P and doxorubicin on perfused vascular volume*

A significant reduction in perfused tumour vasculature was observed following treatment of mice with either OXi4503/CA1P alone or OXi4503/CA1P in combination with doxorubicin compared to control (Fig. 7A and B; $p = 0.014$). However, there was no synergistic effect on disruption of tumour vasculature when mice were treated with both OXi4503/CA1P and doxorubicin; the percentage of perfused tumour vasculature was the

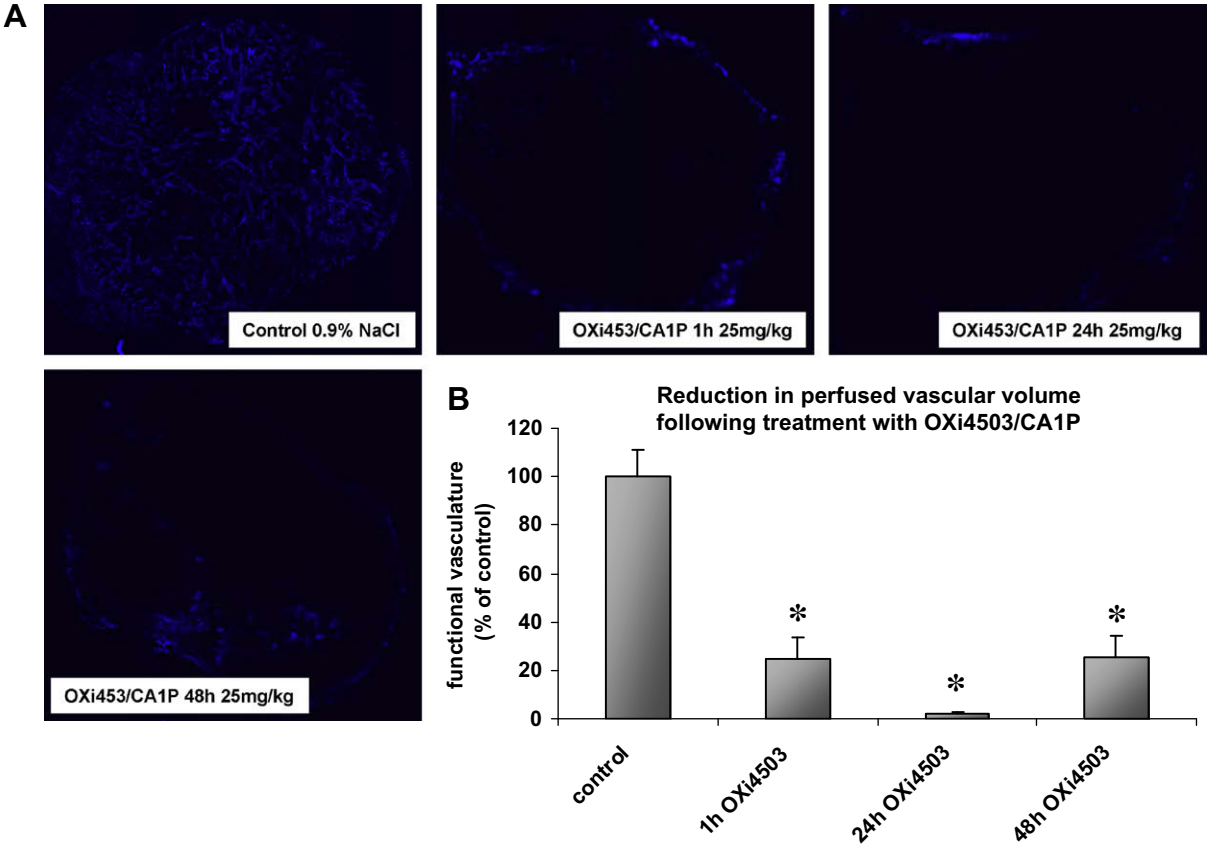

Fig. 4 – (A) A reduction in perfused vasculature (blue staining) of TC-32 tumours after treatment with a single dose of OXi4503/CA1P was observed 1 h post treatment, almost complete shutdown was observed by 24 h. (B) *$p < 0.001$ OXi4503/CA1P compared to control ($n = 4–5$).

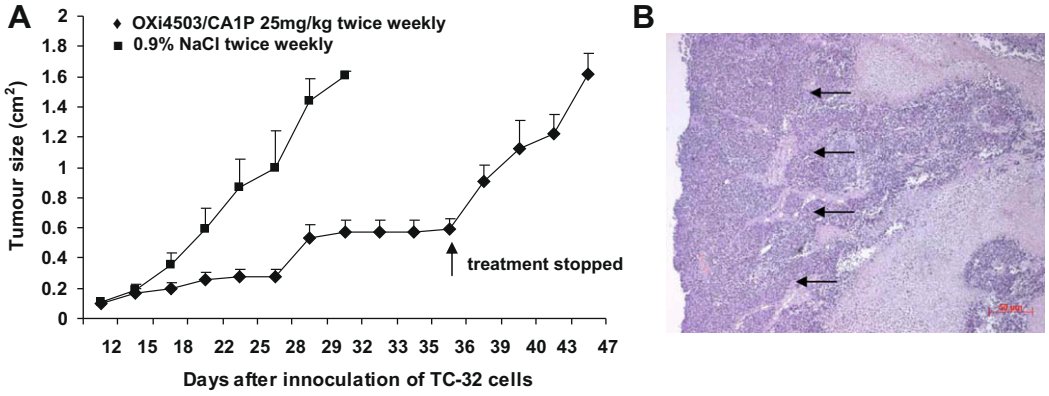

Fig. 5 – (A) Treatment of mice ($n = 5$) with OXi4503/CA1P induced a significant delay ($p < 0.001$) in tumour growth. However, when treatment was stopped all tumours rapidly re-grew reaching >1.4 cm^2 within 10 days. (B) Regrowth of viable proliferative rim of tumour cells (↑). ×40 Magnification.

same as that observed following treatment of mice with OXi4503/CA1P alone (Fig. 7B). Doxorubicin alone appeared to increase perfused vascular volume, although this was not statistically significant.

4. Discussion

OXi4503/CA1P delayed subcutaneous growth of ESFT in nude mice. Consistent with the observations in mice with other

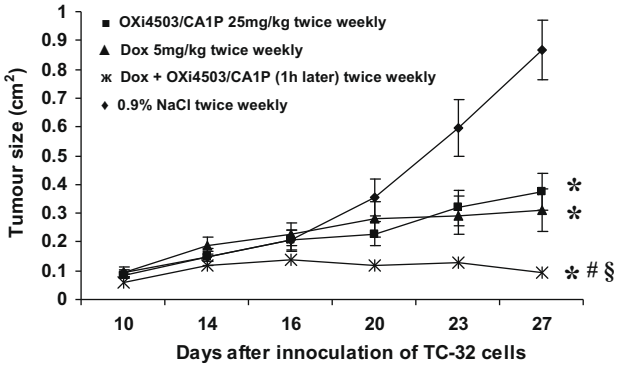

Fig. 6 – Combined effect of OXi4503/CA1P and doxorubicin on the growth of TC-32 tumours. Synergistic growth inhibition was observed in mice treated with doxorubicin and OXi4503/CA1P. *$p < 0.001$ OXi4503/CA1P, doxorubicin, doxorubicin + OXi4503/CA1P versus control; #$p = 0.002$ doxorubicin + OXi4503/CA1P versus OXi4503/CA1P; §$p = 0.03$ doxorubicin + OXi4503/CA1P versus doxorubicin

tumour types,[9,14,15] ESFT from mice treated with OXi4503/CA1P contained large areas of central necrosis surrounded by a rim of viable and proliferating tumour cells. In contrast, no significant delay in tumour growth was observed following treatment of mice with CA4P or OXi8007. CA4P has previously been shown to have no effect in the subcutaneous growth model of human epithelial ovarian carcinoma,[23] although previous reports have demonstrated tumour growth delay in other tumour groups.[8,14,15,24] Differences in the number of alpha-smooth muscle actin (α-SMA)-positive supporting perivascular structures such as pericytes, myofibroblasts and vascular smooth muscle cells may influence the susceptibility of ESFT to VDAs compared to other tumour types.[25]

Rapid occlusion of blood vessels and development of tumour necrosis after a single injection with CA4P, OXi8007 and in particular OXi4503/CA1P are consistent with the reported effects of tubulin-binding agents.[8,9,15,23,26] The increased activity of OXi4503/CA1P observed here compared to the activity of CA4P or OXi8007 may in part be explained by the generation of an ortho-quinone metabolite,[27] which may have a direct effect on ESFT cells in addition to its activity as a tubulin-binding agent.

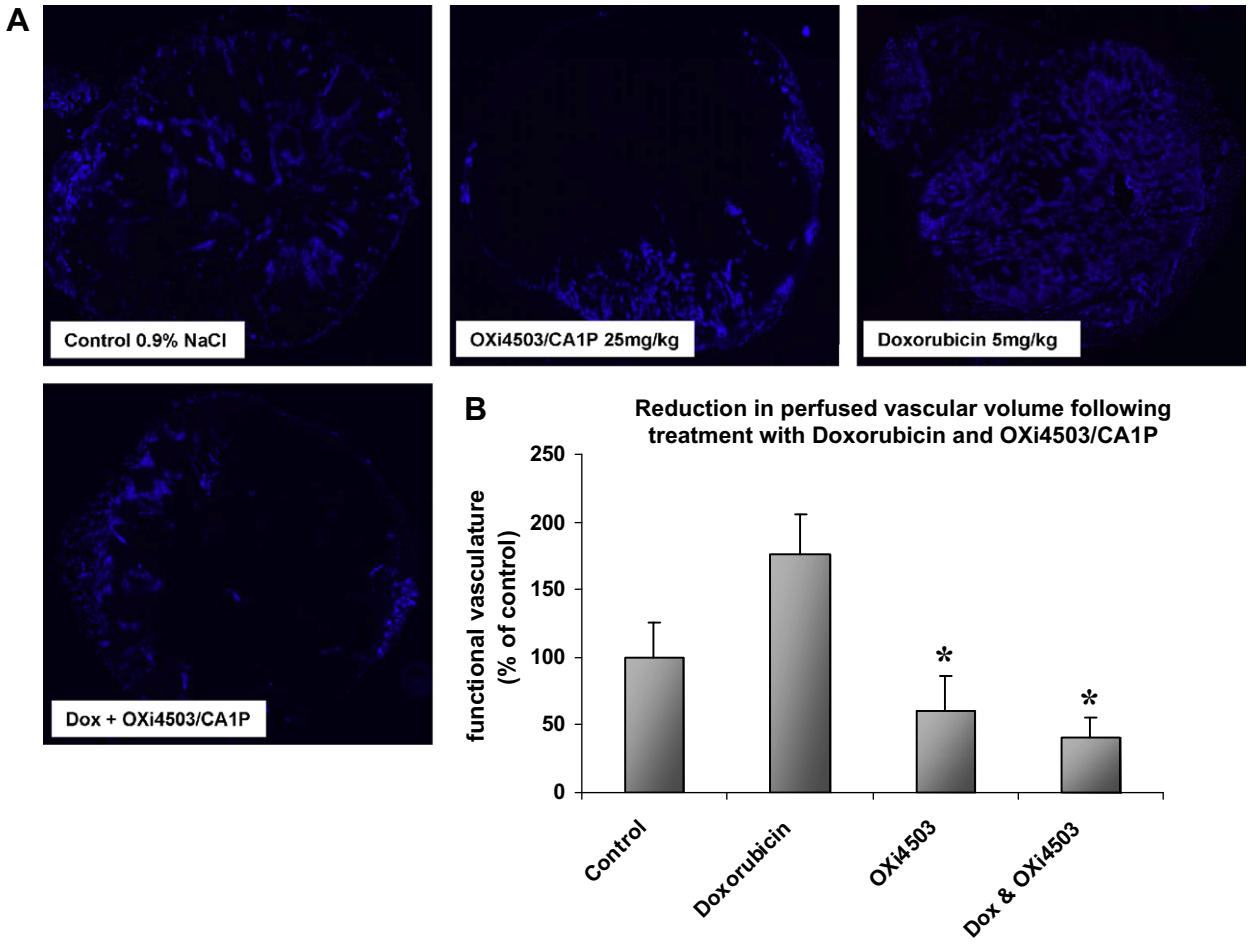

Fig. 7 – (A) Perfused vasculature (blue staining) was reduced in TC-32 tumours 48 h after treatment of mice with a single dose of OXi4503/CA1P alone or in combination with doxorubicin. Doxorubicin alone had no effect on perfused vascular volume. (B) *$p = 0.014$ OXi4503/CA1P, doxorubicin + OXi4503/CA1P versus control ($n = 5$).

Although OXi4503/CA1P rapidly (within 1 h) disrupts the functional vasculature of subcutaneous ESFT, the presence of smaller blood vessels 48 h post initial treatment suggests that neovascularisation may account for some of the recovery in tumour growth observed. Assessing vasculature using immunohistochemistry for CD31 to determine MVD in contrast to Hoechst dye to examine perfused vascular volume confirms the limitations of using CD31 as a marker for assessing changes in vasculature within the tumours. Despite almost complete vascular shutdown at 24 h (observed by staining with Hoechst dye), a change in MVD was not observed. Although MVD has been reported to be a useful prognostic indicator in a number of tumour types, its value as an indicator of the efficacy of vascular-targeting therapies is limited.[28] At the time points evaluated, no apoptotic endothelial cells were observed and apoptosis of tumour cells was confined to regions adjacent to the areas of necrosis. The appearance of apoptotic endothelial cells has previously been described as early as 1–3 h following treatment of MHEC5-T haemangioendothelioma in SCID mice with OXi4503/CA1P.[26] Although not investigated in the current study, it is likely that in subcutaneously growing ESFT endothelial cell death occurred either by apoptosis prior to vascular shutdown at 24 h or via alternative cell death pathways.[25]

Despite the promising effects of OXi4503/CA1P on subcutaneous tumour growth, a viable rim of proliferating tumour cells persisted following treatment. These observations are consistent with those reported in a murine model of colorectal carcinoma liver metastases.[29] Following the withdrawal of OXi4503/CA1P, rapid re-growth of tumours occurred. Interestingly, the majority of tumour cells and the endothelial lining of blood vessels within the viable rim after treatment with OXi4503/CA1P were hypoxic. Such hypoxic conditions may play a crucial role in repopulating tumours by stimulating the process of angiogenesis, upregulating pro-angiogenic factors such as VEGF. We therefore hypothesised that the antitumour efficacy of OXi4503/CA1P might be increased if mice were treated with OXi4503/CA1P plus the anthracycline antibiotic doxorubicin, commonly used in the treatment of ESFT. Combination treatment resulted in a synergistic delay in tumour growth, reflecting the doxorubicin-induced decrease in viable cells at the periphery of the tumour. These observations are consistent with the synergistic effects of CA1P with carboplatin and paclitaxel in a SCID model of human ovarian carcinoma.[23] Despite the effectiveness of combined treatment in our study, prolonged combined treatment (beyond two weeks) was not well tolerated by the mice, suggesting that further optimisation is required. Indeed optimising the dosing, timing and schedule of such combined therapies in preclinical mouse models remains a major challenge in this field.

Further investigations using Hoechst dye to examine perfused vascular volume revealed that the combination treatment with doxorubicin had no greater effect on vascular shutdown than that observed with OXi4503/CA1P alone. This is consistent with the hypothesis that the dominant effect on vascular shutdown was that of OXi4503/CA1P and the enhanced efficacy of the combination treatment was attributed to a direct effect of doxorubicin on tumour cells. The induction of hypoxia following treatment with OXi4503/CA1P might also be exploited for therapeutic advantage by using it in combination with bio-reductive anti-tumour prodrugs that target the hypoxic cells, or preferentially release a therapeutic entity under hypoxic conditions. Although this is an attractive strategy, the optimal approach for scheduling such agents in combination treatment is not obvious but worthy of further investigation.

This study demonstrates that the VDA OXi4503/CA1P slows subcutaneous ESFT growth. In combination with conventional cytotoxic agents or hypoxia-activated prodrugs this may provide a novel therapeutic strategy to treat ESFT.

Conflict of interest statement

None declared.

Acknowledgements

The authors thank OXiGENE Inc. for providing the compounds and funding the mouse studies. The authors also thank the staff at Biological Resources, Clare Hall, Cancer Research UK, London, and Dr. Steve Shnyder and Mrs. Patricia Cooper at the University of Bradford for assistance with *in vivo* experiments, and Sally Jackson and Andrea Berry from the Candlelighters's Children's Cancer Research Group for technical assistance. SD was funded by the Candlelighter's Trust, Leeds, United Kingdom.

REFERENCES

1. Burchill SA, Roberts P. Molecular and genetic abnormalities in tumours of the Ewing's sarcoma family of tumours (ESFT). In: Sherbet GV editor. *The Molecular and Cellular Pathology of Cancer Progression and Prognosis*. Research Signpost; 2006. p. 221–34.
2. Lewis I, Burchill SA, Souhami R. Ewing's sarcoma and the Ewing family of tumours. In: Tannock I, Hohenberger P, Horiot J-C, editors. *Oxford textbook of oncology*. Oxford University Press; 2002. p. 539–51.
3. Hendershot E. Treatment approaches for metastatic Ewing's sarcoma: a review of the literature. *J Pediatr Oncol Nurs* 2005;**22**:339–52.
4. Ahrens SC, Hoffmann C, Jabar S, et al. Evaluation of prognostic factors in a tumor volume-adapted treatment strategy for localized Ewing sarcoma of bone: the CESS 86 experience. Cooperative Ewing Sarcoma Study. *Med Pediatr Oncol* 1999;**32**:186–95.
5. Rodriguez-Galindo C, Spunt SL, Pappo AS. Treatment of Ewing sarcoma family of tumors: current status and outlook for the future. *Med Pediatr Oncol* 2003;**40**:276–87.
6. Folkman J. What is the evidence that tumors are angiogenesis dependent? *J Natl Cancer Inst* 1990;**82**:4–6.
7. Tozer GM, Kanthou C, Baguley BC. Disrupting tumour blood vessels. *Nat Rev Cancer* 2005;**5**:423–35.
8. Grosios K, Holwell SE, McGown AT, Pettit GR, Bibby MC. In vivo and in vitro evaluation of combretastatin A-4 and its sodium phosphate prodrug. *Br J Cancer* 1999;**81**:1318–27.
9. Hill SA, Toze GM, Pettit GR, Chaplin DJ. Preclinical evaluation of the antitumour activity of the novel vascular targeting agent Oxi 4503. *Anticancer Res* 2002;**22**:1453–8.

10. Galbraith SM, Chaplin DJ, Lee F, et al. Effects of combretastatin A4 phosphate on endothelial cell morphology in vitro and relationship to tumour vascular targeting activity in vivo. *Anticancer Res* 2001;**21**:93–102.
11. Tozer GM, Prise VE, Wilson J, Cemazar M, Shan S, Dewhirst MW, et al. Mechanisms associated with tumor vascular shut-down induced by combretastatin A-4 phosphate: intravital microscopy and measurement of vascular permeability. *Cancer Res* 2001;**61**:6413–22.
12. Chaplin DJ, Pettit GR, Hill SA. Anti-vascular approaches to solid tumour therapy: evaluation of combretastatin A4 phosphate. *Anticancer Res* 1999;**19**:189–95.
13. Pettit GR, Lippert 3rd JW. Antineoplastic agents 429. Syntheses of the combretastatin A-1 and combretastatin B-1 prodrugs. *Anticancer Drug Des* 2000;**15**:203–16.
14. Holwell SE, Cooper PA, Thompson MJ, et al. Anti-tumor and anti-vascular effects of the novel tubulin-binding agent combretastatin A-1 phosphate. *Anticancer Res* 2002;**22**:3933–40.
15. Hua J, Sheng Y, Pinney KG, et al. Oxi4503, a novel vascular targeting agent: effects on blood flow and antitumor activity in comparison to combretastatin A-4 phosphate. *Anticancer Res* 2003;**23**:1433–40.
16. Pinney KG, Wang F, Hadimani M. *Indole-containing and combretastatin-related anti-mitotic and anti-tubulin polymerization agents*. 2005; US Patent 6849656.
17. Simpson A, Grimer R, Mangham C, Cullinane C, Lewis I, Burchill SA. MVD predicts disease-free and overall survival in tumours of the Ewing's sarcoma family (ESFT). *Br J Cancer* 2002;**86**:S95.
18. Dalal S, Berry AM, Cullinane CJ, et al. Vascular endothelial growth factor: a therapeutic target for tumors of the Ewing's sarcoma family. *Clin Cancer Res* 2005;**11**:2364–78.
19. Landuyt W, Verdoes O, Darius DO, et al. Vascular targeting of solid tumours: a major 'inverse' volume-response relationship following combretastatin A-4 phosphate treatment of rat rhabdomyosarcomas. *Eur J Cancer* 2000;**36**:1833–43.
20. Hense HW, Ahrens S, Paulussen M, Lehnert M, Jürgens H. Factors associated with tumor volume and primary metastases in Ewing tumors: results from the (EI)CESS studies. *Ann Oncol* 1999;**10**:1073–7.
21. UKCCCR. United Kingdom Co-ordinating Committee on Cancer Research (UKCCCR) Guidelines for the Welfare of Animals in Experimental Neoplasia. 2nd ed. *Br J Cancer* 1998;**77**:1–10.
22. Smith KA, Hill SA, Begg AC, Denekamp J. Validation of the fluorescent dye Hoechst 33342 as a vascular space marker in tumours. *Br J Cancer* 1988;**57**:247–53.
23. Staflin K, Järnum S, Hua J, Honeth G, Kannisto P, Lindvall M. Combretastatin A-1 phosphate potentiates the antitumor activity of carboplatin and paclitaxel in a severe combined immunodeficiency disease (SCID) mouse model of human ovarian carcinoma. *Int J Gynecol Cancer* 2006;**16**:1557–64.
24. Prise VE, Honess DJ, Stratford MR, Wilson J, Tozer GM. The vascular response of tumor and normal tissues in the rat to the vascular targeting agent, combretastatin A-4-phosphate, at clinically relevant doses. *Int J Oncol* 2002;**1**:717–26.
25. Tozer GM, Kanthou C, Parkins CS, Hill SA. The biology of the combretastatins as tumour vascular targeting agents. *Int J Exp Pathol* 2002;**83**:21–38.
26. Sheng Y, Hua J, Pinney KG, Garner CM, et al. Combretastatin family member OXi4503 induces tumor vascular collapse through the induction of endothelial apoptosis. *Int J Cancer* 2004;**111**:604–10.
27. Kirwan IG, Loadman PM, Swaine DJ, et al. Comparative preclinical pharmacokinetic and metabolic studies of the combretastatin prodrugs combretastatin A4 phosphate and A1 phosphate. *Clin Cancer Res* 2004;**10**:1446–53.
28. Hlatky L, Hahnfeldt P, Folkman J. Clinical application of antiangiogenic therapy: microvessel density, what it does and doesn't tell us. *J Natl Cancer Inst* 2002;**94**:883–93.
29. Chan LS, Malcontenti-Wilson C, Muralidharan V, Christophi C. Effect of vascular targeting agent Oxi4503 on tumor cell kinetics in a mouse model of colorectal liver metastasis. *Anticancer Res* 2007;**27**:2317–23.